EUROPEAN ORGANIZATION FOR NUCLEAR RESEARCH

CERN-EP/89-133
October 13, 1989

Measurement of the Z^0 Mass and Width with the OPAL Detector at LEP

The OPAL Collaboration

M.Z. Akrawy[11], G. Alexander[21], J. Allison[14], P.P. Allport[5], K.J. Anderson[8], J.C. Armitage[6], G.T.J. Arnison[18], P. Ashton[14], G. Azuelos[16], J.T.M. Baines[14], A.H. Ball[15], J. Banks[14], G.J. Barker[11], R.J. Barlow[14], J.R. Batley[5], G. Bavaria[16], C. Beard[7], F. Beck[7], K.W. Bell[18], G. Bella[21], S. Bethke[10], O. Biebel[3], I.J. Bloodworth[1], P. Bock[10], H. Boerner[7], H. Breuker[7], R.M. Brown[18], R. Brun[7], A. Buijs[7], H.J. Burckhart[7], P. Capiluppi[2], R.K. Carnegie[6], A.A. Carter[11], J.R. Carter[5], C.Y. Chang[15], D.G. Charlton[7], J.T.M. Chrin[14], I. Cohen[21], J.E. Conboy[13], M. Couch[1], M. Coupland[12], M. Cuffiani[2], S. Dado[20], G.M. Dallavalle[13], O.W. Davies[14], M.M. Deninno[2], A. Dieckmann[10], M. Dittmar[4], M.S. Dixit[17], D. Duchesneau[16], E. Duchovni[24], I.P. Duerdoth[7,c], D. Dumas[6], H. El Mamouni[16], P.A. Elcombe[5], P.G. Estabrooks[6], F. Fabbri[2], P. Farthouat[19], H.M. Fischer[3], D.G. Fong[15], M.T. French[18], C. Fukunaga[22], B. Gandois[19], O. Ganel[24], J.W. Gary[10], N.I. Geddes[18], C.N.P. Gee[18], C. Geich-Gimbel[3], S.W. Gensler[8], F.X. Gentit[19], G. Giacomelli[2], W.R. Gibson[11], J.D. Gillies[18], J. Goldberg[20], M.J. Goodrick[5], W. Gorn[4], D. Granite[20], E. Gross[24], P. Grosse-Wiesmann[7], J. Grunhaus[21], H. Hagedorn[9], J. Hagemann[7], M. Hansroul[7], C.K. Hargrove[17], J. Hart[5], P.M. Hattersley[1], D. Hatzifotiadou[7], M. Hauschild[7], C.M. Hawkes[7], E. Heflin[4], J. Heintze[10], R.J. Hemingway[6], R.D. Heuer[7], J.C. Hill[5], S.J. Hillier[1], P.S. Hinde[14], C. Ho[4], J.D. Hobbs[8], P.R. Hobson[23], D. Hochman[24], B. Holl[7], R.J. Homer[1], S.R. Hou[15], C.P. Howarth[13], R.E. Hughes-Jones[14], P. Igo-Kemenes[10], M. Imori[22], D.C. Imrie[23], A. Jawahery[15], P.W. Jeffreys[18], H. Jeremie[16], M. Jimack[7], E. Jin[4,b], M. Jobes[1], R.W.L. Jones[11], P. Jovanovic[1], D. Karlen[6], K. Kawagoe[22], T. Kawamoto[22], R.G. Kellogg[15], B.W. Kennedy[13], C. Kleinwort[7], D.E. Klem[17], G. Knop[3], T. Kobayashi[22], L. Koepke[7], T.P. Kokott[3], M. Koshiba[22], R. Kowalewski[6], H. Kreutzmann[3], J. von Krogh[10], J. Kroll[8], P. Kyberd[11], G.D. Lafferty[14], F. Lamarche[16], W.J. Larson[4], M.M.B. Lasota[11], J.G. Layter[4], P. Le Du[19], P. Leblanc[16], D. Lellouch[7], P. Lennert[10], L. Lessard[16], L. Levinson[24], S.L. Lloyd[11], F.K. Loebinger[14], J.M. Lorah[15], B. Lorazo[16], M.J. Losty[17], J. Ludwig[9], N. Lupu[20], J. Ma[4,b], A.A. Macbeth[14], M. Mannelli[7], S. Marcellini[2], G. Maringer[3], J.P. Martin[16], T. Mashimo[22], P. Mättig[7], U. Maur[3], T.J. McMahon[1], A.C. McPherson[6], F. Meijers[7], D. Menszner[10], F.S. Merritt[8], H. Mes[17], A. Michelini[7], R.P. Middleton[18], G. Mikenberg[24], D.J. Miller[13], C. Milstene[21], M. Minowa[22], W. Mohr[9], A. Montanari[2], T. Mori[22], M.W. Moss[14], A. Muller[19], P.G. Murphy[14], W.J. Murray[5], B. Nellen[3], H.H. Nguyen[8], M. Nozaki[22], A.J.P. O'Dowd[14], S.W. O'Neale[7,d], B. O'Neill[4], F.G. Oakham[17], F. Odorici[2], M. Ogg[6], H. Oh[4], M.J. Oreglia[8], S. Orito[22], G.N. Patrick[18], S.J. Pawley[14], A. Perez[24], J.E. Pilcher[8], J.L. Pinfold[24], D.E. Plane[7], B. Poli[2], A. Possoz[8,e], A. Pouladdej[6], T.W. Pritchard[11], G. Quast[7], J. Raab[7], M.W. Redmond[8], D.L. Rees[1], M. Regimbald[16], K. Riles[4], C.M. Roach[5], F. Roehner[9], A. Rollnik[3], J.M. Roney[8], A.M. Rossi[2,a], P. Routenburg[6], K. Runge[9], O. Runolfsson[7], S. Sanghera[6], R.A. Sansum[18],

M. Sasaki[22], B.J. Saunders[18], A.D. Schaile[9], O. Schaile[9], W. Schappert[6], P. Scharff-Hansen[7], H. von der Schmitt[10], S. Schreiber[3], J. Schwarz[9], A. Shapira[9,f], B.C. Shen[4], P. Sherwood[13], A. Simon[3], G.P. Siroli[2], A. Skuja[15], A.M. Smith[7], T.J. Smith[1], G.A. Snow[15], E.J. Spreadbury[13], R.W. Springer[15], M. Sproston[18], K. Stephens[14], H.E. Stier[9], R. Ströhmer[10], D. Strom[8], H. Takeda[22], T. Takeshita[22], T. Tsukamoto[22], M.F. Turner[5], G. Tysarczyk[10], D. Van den plas[16], G.J. VanDalen[4], C.J. Virtue[17], A. Wagner[10], C. Wahl[9], H. Wang[4,b], C.P. Ward[5], D.R. Ward[5], J. Waterhouse[6], P.M. Watkins[1], A.T. Watson[1], N.K. Watson[1], M. Weber[10], S. Weisz[7], N. Wermes[7], M. Weymann[9], G.W. Wilson[7], J.A. Wilson[1], I. Wingerter[7], V-H. Winterer[9], N.C. Wood[13], S. Wotton[7], B. Wuensch[3], T.R. Wyatt[14], R. Yaari[24], H. Yamashita[22], Y. Yang[4,b], G. Yekutieli[24], W. Zeuner[7], G.T. Zorn[15], S. Zylberajch[19].

[1]School of Physics and Space Research, University of Birmingham, Birmingham, B15 2TT, UK
[2]Dipartimento di Fisica dell' Universita di Bologna and INFN, Bologna, 40126, Italy
[3]Universität Bonn, D-5300 Bonn 1, FRG
[4]Department of Physics, University of California, Riverside, CA 92521 USA
[5]Cavendish Laboratory, Cambridge, CB3 0HE, UK
[6]Carleton University, Dept of Physics, Colonel By Drive, Ottawa, Ontario K1S 5B6, Canada
[7]CERN, European Organisation for Particle Physics, 1211 Geneva 23, Switzerland
[8]Enrico Fermi Institute and Dept of Physics, University of Chicago, Chicago Illinois 60637, USA
[9]Fakultät für Physik, Albert Ludwigs Universität, D-7800 Freiburg, FRG
[10]Physikalisches Institut, Universität Heidelberg, D-6900 Heidelberg, FRG
[11]Queen Mary and Westfield College, University of London, London, E1 4NS, UK
[12]Birkbeck College, London, WC1E 7HV, UK
[13]University College London, London, WC1E 6BT, UK
[14]Department of Physics, Schuster Laboratory, The University, Manchester M13 9PL, UK
[15]Dept. of Physics and Astronomy, University of Maryland, College Park, Maryland 20742, USA
[16]Laboratoire de Physique Nucleaire, Universite de Montreal, Montreal, Quebec, H3C 3J7, Canada
[17]National Research Council, Herzberg Institute of Astrophysics, Ottawa, Ont. K1A 0R6, Canada
[18]Rutherford Appleton Laboratory, Chilton, Didcot, Oxfordshire, OX11 0QX, UK
[19]DPhPE, CEN Saclay, F-91191 Gif-sur-Yvette France
[20]Department of Physics, Technion-Israel Institute of Technology, Haifa 32000, Israel
[21]Department of Physics and Astronomy, Tel Aviv University, Tel Aviv 69978, Israel
[22]Int. Center for Elementary Particle Phys. and Dept. of Phys., Univ. of Tokyo, Tokyo 113, Japan
[23]Brunel University, Uxbridge, Middlesex, UB8 3PH ,UK
[24]Nuclear Physics Department, Weizmann Institute of Science, Rehovot, 76100, Israel

[a]Present address: Dipartimento di Fisica, Universita della Calabria, 87036 Rende, Italy
[b]On leave from Harbin Institute of Technology, Harbin, China
[c]On leave from Manchester University
[d]On leave from Birmingham University
[e]Present address: EPFL, Lausanne
[f]On leave from Weizmann Institute

(Submitted to Physics Letters)

Abstract

We report an experimental determination of the cross section for $e^+e^- \rightarrow$ hadrons from a scan around the Z^0 pole. On the basis of 4350 hadronic events collected over seven energy points between 89.26 GeV and 93.26 GeV we obtain a mass of $m_Z = 91.01 \pm 0.05 \pm 0.05$ GeV, and a total decay width of $\Gamma_Z = 2.60 \pm 0.13$ GeV. In the context of the standard model these results imply 3.1 ± 0.4 neutrino generations.

One of the major achievements in elementary particle physics over the past two decades has been the unification of weak and electromagnetic interactions and the development of the standard model [1]. An essential element of the unification is the Z^0 boson, the massive neutral carrier of the electroweak field, discovered at CERN [2]. This paper reports a precise determination of the mass and width of the Z^0. The mass is one of the fundamental parameters of the standard model while the width reflects the coupling of the Z^0 to all known fundamental particles.

The data were recorded at the CERN e^+e^- collider, LEP, during its first 15 days of operation for physics and correspond to an integrated luminosity of ~ 190 nb^{-1}. These measurements used the OPAL detector [3], which is a multipurpose apparatus with excellent acceptance for Z^0 decays over a solid angle of nearly 4π. The detector consists of a system of central tracking chambers inside a solenoid which provides a uniform magnetic field of 0.435 T. The solenoid coil is surrounded by a time-of-flight counter array, a lead glass electromagnetic calorimeter with a presampler, an instrumented magnet return yoke serving as a hadron calorimeter and four layers of outer muon chambers. A forward detector serves as a luminosity monitor. The measurement described here primarily exploits the electromagnetic calorimeter, the time-of-flight system, the tracking chambers, and the forward detector.

The central tracking detector is divided into a precision vertex chamber, a large volume jet chamber and a z − chamber. The main tracking is done with the jet chamber, a drift chamber of approximately four metre length and two metre radius with 159 layers of wires, providing both high redundancy and precision for the reconstruction of multihadronic events. During the data taking the jet chamber is switched off for short periods when the beams are unstable or the background rates are high. The time-of-flight system covers the barrel region $|\cos\theta| \leq 0.82$, where θ is the polar angle with respect to the beam direction. It consists of 160 scintillator bars, 6.8 m long and 45 mm thick, located at a radius of 2.4 m. The main electromagnetic calorimeter consists of a cylindrical array of 9,440 lead glass blocks of 24.6 radiation lengths thickness, covering the polar angular range of $|\cos\theta| < 0.82$, and 2,264 lead glass blocks of 20 radiation lengths thickness in the endcaps, covering the polar angular region between $0.81 < |\cos\theta| < 0.98$. The blocks each subtend a solid angle of approximately 40×40 mrad^2 and project towards the interaction point in the barrel region and along the beam direction in the endcaps. The two sections of the electromagnetic calorimeter together cover 98% of the solid angle.

The luminosity of the colliding beams was determined by observing small angle Bhabha scattering with the forward detector. This device consists of two identical elements placed around the beam pipe at either end of the central tracking detector. Its acceptance covers angles from 40 to 150 mrad from the beam and 2π in azimuth. At the Z^0 peak the Bhabha cross section in this region is about 70 nb, with 0.3% contamination from e^+e^- decays of the Z^0 itself. The main element of the forward detector for this analysis was a lead-scintillator calorimeter of 26 radiation lengths thickness, divided into 16 azimuthal segments. The first 4 radiation lengths of the calorimeter are used as a presampler and are read out separately. A set of proportional-tube chambers are located between the presampler and the main calorimeter. The radial position of showers in the calorimeter is obtained by independent light readout from the inner and outer edges of the main calorimeter while the tube chambers are used to calibrate this measurement. The accuracy is 3 mm at the inner edge and 25 mm near the outside. The azimuthal position is obtained to approximately 3 degrees from energy sharing between segments.

The trigger for hadronic decays of the Z^0 is based mainly on the information from three independent detector components: the electromagnetic calorimeter, the time-of-flight system (TOF) and the jet chamber. The calorimeter trigger requires an energy sum of at least 6 GeV in the lead glass barrel or in one endcap, while the TOF trigger requires hits in at least three nonadjacent

time-of-flight counters. An independent element for triggering on charged particles is provided by the track trigger of the jet chamber. Here at least two tracks are required to originate from the vertex in the r-z projection with a minimum transverse momentum of 450 MeV/c.

The forward detector triggered the readout if more than 12 GeV was deposited on each side in a back-to-back configuration of adjacent main calorimeter segments, or if more than 15 GeV was observed on each side without the back-to-back requirement.

The offline selection of multihadron events used principally the electromagnetic calorimeter and the time-of-flight system. The following requirements defined a multihadron candidate: (i) at least 10 clusters of lead glass blocks with at least 100 MeV in each cluster, (ii) a total energy in the lead glass of at least 10% of the centre of mass energy and (iii) an energy balance,

$$\mid R_{bal} \mid = \mid \Sigma(E_{clus} \cdot \cos\theta) \mid / \Sigma E_{clus} \leq 0.65$$

where E_{clus} is the energy per cluster. In order to reject background consisting mainly of cosmic rays, it was also required that events with at least 50% of the observed energy seen in the barrel have at least four time-of-flight counters fired within $\pm$ 8 nsec of the expected arrival time.

Figure 1 shows the effect of these cuts on the data after this last requirement on the time-of-flight counters. Figure 1a displays the distribution of the fraction of the centre-of-mass energy seen, $R_{vis} = \Sigma E_{clus}/E_{cm}$, versus the cluster multiplicity N_{clus}. The hadronic sample with both large R_{vis} and large N_{clus} is clearly separated from the bulk of the background from e^+e^- decays ($R_{vis} = 1$, low cluster multiplicity), τ - pairs (medium R_{vis} and low cluster multiplicity) and from other background such as cosmic rays (low R_{vis}). Figure 1b shows the effect of the energy balance cut after selecting events with $N_{clus} \geq 10$. The multihadron sample, with small values for the energy balance and large R_{vis}, is clearly differentiated from background events, characterised by lower R_{vis} and a wide spread of the energy balance. The projection of the R_{vis} distribution after cuts in the energy balance is shown in fig. 1c. The histogram shows for comparison the results of a Monte Carlo simulation of multihadron events [4]. The agreement is satisfactory for R_{vis} larger than the required value of 0.1.

The background contamination of the sample has been estimated by several methods. Monte Carlo calculations were used to predict the background from two photon processes, and from electron-pair and τ-pair decays of the Z^0. These backgrounds are predicted to be $< 0.1\%$, $< 0.1\%$, and 0.3% respectively. A sample of 819 events taken on the Z^0 peak was scanned. For 540 of these events full information from the jet chamber was available. The scan searched for beam-gas or beam-wall interactions and for cosmic rays and τ decays. Three τ decays were observed and no other background. A second visual scan examined multihadron candidates with a reconstructed vertex more than $\pm$50 cm from the interaction vertex and concluded that beam-gas or beam-wall background is $\leq 0.1\%$. Finally, a sample of data was analysed for which there was no beam in the storage ring. From these studies one estimates an upper limit of 1 cosmic ray event in the sample and an overall background of 0.3%, arising almost entirely from τ decays.

To calculate the acceptance of the detection and event selection procedure, the process $e^+e^- \rightarrow (Z^0, \gamma) \rightarrow q\bar{q}$ with subsequent hadronization was simulated using the JETSET parton shower model with five flavours and string fragmentation [4]. The generated events formed the input to a detector simulation which included full showering and interactions in the detector. In this process, raw data such as drift times and pulse heights were simulated and passed through the same reconstruction and selection procedures as the actual data. An acceptance of 98.2$\pm$0.2% was calculated for multihadronic events. Various checks have been made to estimate the uncertainty in the acceptance. There is good agreement between the model predictions and the properties of the

multihadronic sample (see, for example fig. 1c). Furthermore, variations in calculated acceptance caused by using different parameters for the JETSET model or the HERWIG hadronization model [5] have been studied. Based on these results, the overall systematic error on the value for the acceptance is estimated to be 1%.

To provide a further check of systematic uncertainties in efficiency and backgrounds, a multihadron sample was selected using full reconstruction of the information provided by the jet chamber. This was available for approximately 75% of the data. Cuts similar to (i) and (ii) of the previous selection were used together with the requirement of at least 5 tracks from the interaction vertex. The event sample selected under these conditions agrees to better than 1% with the event sample selected without tracking information.

As another check, the final multihadron sample was compared with that obtained from an independent online selection using different algorithms for cluster finding. The overlap was checked at each energy point and found to coincide with the full off line analysis to better than 1%.

The overall trigger efficiency for hadronic decays which pass the acceptance criteria is determined from the redundancy between the three main trigger modes. The trigger efficiency using the electromagnetic energy is found to be $\geq$ 99.5% for an energy deposit of more than 7 GeV in the barrel part and $\geq$ 99% in the endcap for an energy deposit of more than 12 GeV. The trigger using the time-of-flight system is more than 99.8 % efficient for events with jets pointing into the barrel region and 87% efficient for events with jets pointing into the endcaps. The track trigger itself is more than 99% efficient but was not active for part of the data taking. On the basis of these measurements and a detailed Monte Carlo simulation of the electromagnetic energy trigger an overall trigger efficiency of $>$ 99.5% is obtained. The dependence on the center-of-mass energy was found to be less than 0.1%.

Since the systematic errors on the luminosity dominate all other errors in this study, special care is required in its analysis. Bhabha events were selected by requiring a reconstructed cluster in each end of the forward detector with at least 55% of the beam energy and a coplanarity angle $\Delta\phi$ in the interval 180$\pm$20 degrees. Figures 2a and 2b show how the energy requirement eliminates the intermittent background of chance electron-positron coincidences. Based on an examination of the full set of such plots at all beam energies, the estimated background contamination is less than 0.1%.

The detector acceptance corresponding to the above requirements was determined using the RADBAB generator [6] in a detailed Monte Carlo simulation of electromagnetic showers within the detector and surrounding material. The validity of the Monte Carlo was established by comparison with test beam data. We estimate that the systematic errors in this calculation are about 5%, arising from residual imperfections in the simulation (4%), limited Monte Carlo statistics (2%), and uncertainties in the trigger efficiency (1.5%), beam position (2%), and treatment of radiative corrections (1%).

As a check on systematic errors in the above method, the luminosity was also determined using the measured transverse position of the showers in the calorimeters. A subset of events was used where the average scattering angle from the two ends of the detector was in the interval 60 to 120 mrad. In this region the calorimeter acceptance is unobstructed and the calorimeter position measurements could be calibrated using measurements from the tube chambers. The acceptance was calculated from the non-radiative Bhabha cross section without Monte Carlo simulation. Figure 2c shows the experimentally observed angular distribution and the theoretical curve, normalized to the number of events in the fiducial region. The systematic errors inherent in this method are

estimated to be about 5% in total. Position calibration uncertainties (3%) and resolution effects (3%) represent error sources independent of the errors in the first method, while uncertainties in the trigger efficiency (1.5%), radiative corrections (2%) and beam position (1%), are common to the two methods. For the entire data sample reported here a total of 10482 Bhabha events was observed and the two methods of determining the luminosity agreed to within $1 \pm 1.5\%$.

The hadronic cross section at each centre-of-mass energy is given by the relation

$$\sigma = \frac{1}{\mathcal{L}}\frac{1}{\varepsilon} \cdot (N_{had} - N_b) \tag{1}$$

where $\mathcal{L}$ denotes the integrated luminosity and ε the overall multihadron efficiency, which is the product of the acceptance and the trigger efficiency. N_{had} is the number of events passing the selection criteria for hadronic events, and N_b is the number of background events. The cross section as a function of energy was calculated using a value for the overall efficiency of 97.7 % and a background fraction of 0.3 %. The values obtained are summarised in table 1 and plotted in fig. 3a.

The dominant systematic error on the cross section is that associated with the luminosity measurement, estimated above to be 5 %. Further contributions to the error from the acceptance determination, the background subtraction, and the trigger efficiency are small in comparison. Thus the overall systematic uncertainty in the cross section is 5 %. The point-to-point systematic error, also dominated by the luminosity measurement, is estimated to be 1 %.

An accurate knowledge of the absolute energy of the LEP beams is essential to the determination of the Z^0 mass. Values provided by the LEP Division are listed in Table 1 [7]. These are based on magnetic measurements prior to installation and readings taken during the run of a flip coil in a reference magnet powered in series with the main ring dipoles. Calibrated flux loops installed in the lower pole of all magnets are used to monitor aging effects. A series of corrections have been evaluated. These include the present readings from the flux loops, the influence of the earth's magnetic field, and the effect of a 0.37 mm shift of the real beam position relative to the central orbit. The residual fractional error in the energy of each beam is $5 \cdot 10^{-4}$, corresponding to 45 MeV in the centre-of mass energy. The fractional point-to-point error in the energy is $1 \cdot 10^{-4}$.

In order to determine the mass, m_Z, and width, Γ_Z, of the Z^0, a Breit-Wigner lineshape with s-dependent width was used:

$$\tilde{\sigma}(s) = \sigma_{had}^{pole} \frac{s\Gamma_Z^2}{(s - m_Z^2)^2 + \frac{s^2}{m_Z^2}\Gamma_Z^2}. \tag{2}$$

The overall normalisation is:

$$\sigma_{had}^{pole} = \tilde{\sigma}(s = m_Z^2) = \frac{12\pi}{m_Z^2}\frac{\Gamma_e\,\Gamma_{had}}{\Gamma_Z^2} \tag{3}$$

To account for radiative corrections, $\tilde{\sigma}(s)$ has been convoluted with the initial state radiation spectrum:

$$\sigma(s) = \int_{m_\pi^2}^{s} f(s, s')\,\tilde{\sigma}(s')\,ds'. \tag{4}$$

For the function $f(s, s')$ in equation (4) the calculation of [8] is adopted, which is based on a second order treatment with exponentiation of soft photons. Therefore σ_{had}^{pole} is related to the measured cross section at $s = m_Z^2$ by a factor determined from radiative corrections.

The line shape formula contains three free parameters, m_Z, Γ_Z, and σ_{had}^{pole}. A fit was performed where these three quantities were varied independently. The results are shown as the solid curve in fig. 3a and the resulting values for the parameters are given in line 1 of table 2. From the line shape fit the cross section at $s = m_z^2$ is $\sigma = 30.7$ nb. As can be seen, the quality of the fit to the data is excellent.

In the standard model with three generations the only significant free parameter is m_Z. The values of Γ_Z and σ_{had}^{pole} can be expressed in terms of m_Z, m_{top} and m_{Higgs} [18]. The influence of m_{top} and m_{Higgs} on the line shape is negligible and their values have each been fixed to 100 GeV. The value of α_s also enters and a value of 0.12 has been used. The present experimental uncertainty in α_s introduces an error of about 1% on the calculated widths and cross sections. The result of this standard model fit is shown as the dashed line in fig. 3a and in line 2 of table 2. The data are in good agreement with the expectation of the standard model.

Since (2) is an approximation, the standard model fit based on three generations was repeated including the interference term and the QED term with the full electroweak corrections using the line shape program ZSHAPE [17]. The result is $m_Z = 91.011 \pm 0.052$ GeV which is fully consistent with $m_Z = 91.013 \pm 0.053$ GeV as obtained with formula (2). Thus the conclusions based on the simpler fit are unaltered.

An analysis has been done to investigate the possible existence of additional light neutrino generations. It is assumed that these neutrinos have the standard model coupling and that no other new physics is reflected in the line shape. The total width is written as $\Gamma_Z = \Gamma_Z^{SM} + (N_\nu - 3) \cdot \Gamma_\nu^{SM}$. The quantities m_Z and N_ν are varied but σ_{had}^{pole} is fixed by the relation given in (3). Line 3 of table 2 shows the results. One obtains $N_\nu = 3.12 \pm 0.42$. If expressed as an upper limit the result is $N_\nu < 3.88$ at 90% confidence level or $N_\nu < 4.04$ at 95% confidence level.

Another test of the number of light neutrinos can be made using the model independent fit. As the global correlation coefficient of m_Z is small one can restrict the consideration to contours of the χ^2 statistic in the Γ_Z - σ_{had}^{pole} plane. These are displayed in fig. 3b. The cross shows the best fit to the data and the dot and square the standard model predictions for 3 and 4 light neutrino generations. The small bar through these symbols shows the uncertainty in the predictions when m_{top} is varied from 60-200 GeV and m_{Higgs} from 10-1000 GeV. From our measurements we attribute a probability of 47% for the standard model prediction with $N_\nu = 3$ and a probability of 8% for $N_\nu = 4$.

In conclusion, we have measured the mass of the Z^0 to be $91.01 \pm 0.05 \pm 0.05$ GeV and its total decay width to be 2.60 ± 0.13 GeV. These results are in agreement with the earlier but less precise measurements of Abe et al. [9], Abrams et al. [10], Albajar et al. [11], and Ansari et al. [12]. Our result that $N_\nu < 3.88$ at 90% confidence can be compared with the result of Abrams et al. [10] that $N_\nu < 5.5$ at 90% confidence based on a similar analysis. It is also in agreement with limits on N_ν set by the UA1 [13] and UA2 [12] experiments at the CERN $p\bar{p}$ collider, the ASP [14] and MAC [15] experiments at PEP, and the CELLO experiment [16] at PETRA.

It is a pleasure to thank the LEP Division for the remarkably smooth start-up of the machine, the precise information on the absolute energy, and their continuing close cooperation with our experimental group. In addition to the support staff at our own institutions we are pleased to acknowledge the following: The Bundesministerium für Forschung und Technologie, FRG, The Department of Energy, USA, The Institut de Recherche Fondamentale du Commissariat a l'Energie Atomique, The Israeli Ministry of Science, The Minerva Gesellschaft, The National Science Foundation, USA, The Natural Sciences and Engineering Research Council, Canada, The Japanese Ministry of Education, Science and Culture (the Monbusho) and a grant under the Monbusho

International Science Research Program, The Science and Engineering Research Council, UK and The A. P. Sloan Foundation.

Table 1: Integrated luminosity and event numbers
Listed are the c.m. energies, $\sqrt{s}$ in GeV, the integrated luminosity $\mathcal{L}$ (nb^{-1}), and the number of events N_{ev} remaining after the hadron selection. The hadronic cross sections σ are quoted with their statistical and point-to-point systematic errors. The overall systematic error is 45 MeV on the energy scale and 5 % on the cross section. The point-to-point error on the energy is 10 MeV.

$\sqrt{s}$ (GeV)	$\mathcal{L}(\mathrm{nb}^{-1})$	N_{ev}	σ (nb)
89.26	15.28±0.52	172	11.48 ± 0.97
90.26	20.50±0.61	432	21.49 ± 1.26
91.02	25.42±0.68	785	31.50 ± 1.48
91.26	72.43±1.15	2190	30.84 ± 0.95
92.26	12.51±0.49	263	21.44 ± 1.60
92.51	10.73±0.45	167	15.87 ± 1.42
93.26	29.89±0.76	350	11.94 ± 0.73

Table 2: Results of the fits for the Z^0 resonance parameters described in the text.

Fit	m_Z(GeV)	Γ_Z(GeV)	N_ν	σ^{pole}_{had}(nb)	χ^2/DOF
1	91.010±0.051	2.60±0.13	-	41.7±2.4	3.1/4
2	91.013±0.053	-	-	-	4.7/6
3	91.013±0.053	-	3.12 ± 0.42	-	4.6/5

References

[1] S. Weinberg, Phys. Rev. Lett. 19 (1967) 1264; A. Salam, Elementary Particle Theory, ed. N. Svartholm (Almquist and Wiksells, Stockholm, 1969) p. 367; S. L. Glashow, J. Iliopoulos,and L. Maiani, Phys. Rev. D2 (1970) 1285. For a recent review see: P. Langacker, Status of the Standard Electroweak Model, Proceedings of the XXIV International Conference on High Energy Physics, Munich, (1988).

[2] G. Arnison et al., Phys. Lett. 126B (1983) 398; P. Bagnaia et al., Phys. Lett. 129B 130 (1983).

[3] OPAL Technical proposal (1983) and CERN/LEPC/83-4.

[4] T. Sjostrand, Computer Physics Commun. 39 (1986) 347; JETSET, Version 7.1.

[5] G. Marchesini and B.R. Webber, Nucl. Phys. B310 (1988) 461; HERWIG, Version 3.2.

[6] F.A. Berends, R. Kleiss, W. Hollik, Nucl. Phys. B304 (1988) 712.

[7] J. Billan et al, Calibration of Beam Momentum, LEP Commissioning Note 12, LEP Division, CERN.

[8] F.A. Berends, W.L. Van Neerven, G.J.H Burgers, Nucl. Phys. B297 (1988) 429; see also M. Greco, G. Pancheri-Srivastava, Y. Srivastava, Nucl. Phys. B171 (1980) 118,(E. B197 (1982) 543).

[9] F. Abe et al., Phys. Rev. Lett. 63 (1989) 720.

[10] G.S. Abrams et al., Phys. Rev. Lett. 63 (1989) 724.

[11] C. Albajar et al., CERN–EP/88-168 (to appear in Z. Phys. C).

[12] R. Ansari et al., Phys. Lett. 186B (1987) 440.

[13] C. Albajar et al., Phys. Lett. 185B (1987) 241; C. Albajar et al., Phys. Lett. 198B (1987) 271.

[14] C. Hearty et al., Phys. Rev. D39 (1989) 3207.

[15] W. T. Ford et al., Phys. Rev. D33 (1986) 3472.

[16] H. J. Behrend et al., Phys. Lett. 215B (1988) 186.

[17] W.J.P. Beenakker, F.A. Berends and S.C. van der Marck; Instituut Lorentz, University of Leiden, P.O.B. 9506, 2300 RA Leiden, The Netherlands (1989).

[18] M. Consoli, W. Hollik, F. Jegerlehner, Proceedings of the Workshop on Z^0 Physics at LEP, ed. G. Altarelli, R. Kleiss and C. Verzegnassi (1989).

Figure Captions

FIGURE 1: (a) Number of clusters in the electromagnetic calorimeter, versus the fraction of the c.m. energy measured there, R_{vis}. (b) Longitudinal energy balance $R_{bal} = \Sigma(E_{clus} \cdot \cos\theta) \ / \ E_{vis}$ versus the fraction of energy seen, R_{vis} for $N_{clus} \geq 10$. (c) Distribution of R_{vis} compared with a histogram of the expectation for multihadron events. The number of clusters has been required to be $\geq$ 10 and the longitudinal energy balance to be in the range -0.65 to +0.65. The final multihadron event sample uses events with R_{vis} above 0.1.

FIGURE 2a: Plot of E_{min}, the lower of the two cluster energies for forward detector Bhabha candidates, versus $\Delta\phi$, the coplanarity angle between showers in the two detectors; for the beam energy point with the least background. The lines at 25 GeV and 180$\pm$20 deg represent the cuts. Approximately 1000 events are shown.

FIGURE 2b: Same as fig. 2a but for the beam energy point with the most random-coincidence background. Approximately 1000 events are shown.

FIGURE 2c: The differential distribution of the Bhabha scattering angle θ taken as the average from the determinations at the two ends. The $1/\theta^3$ curve is fit over the region of clean acceptance (60 to 120 mrad).

FIGURE 3a: Measured multihadron cross section versus centre of mass energy. The solid curve is a 3-parameter model independent fit. The dashed curve is the best fit from the standard model where only m_Z is varied.

FIGURE 3b: Contour plot of the χ^2 statistic for the fit to the resonance curve as a function of Γ_Z and σ^{pole}_{had}. Curves correspond to increments of one standard deviation. The cross shows the best fit to the data and the dot and square the standard model predictions for 3 and 4 light neutrino generations. The small bar through these symbols shows the uncertainty in the predictions when m_{top} is varied from 60-200 GeV and m_{Higgs} from 10-1000 GeV.

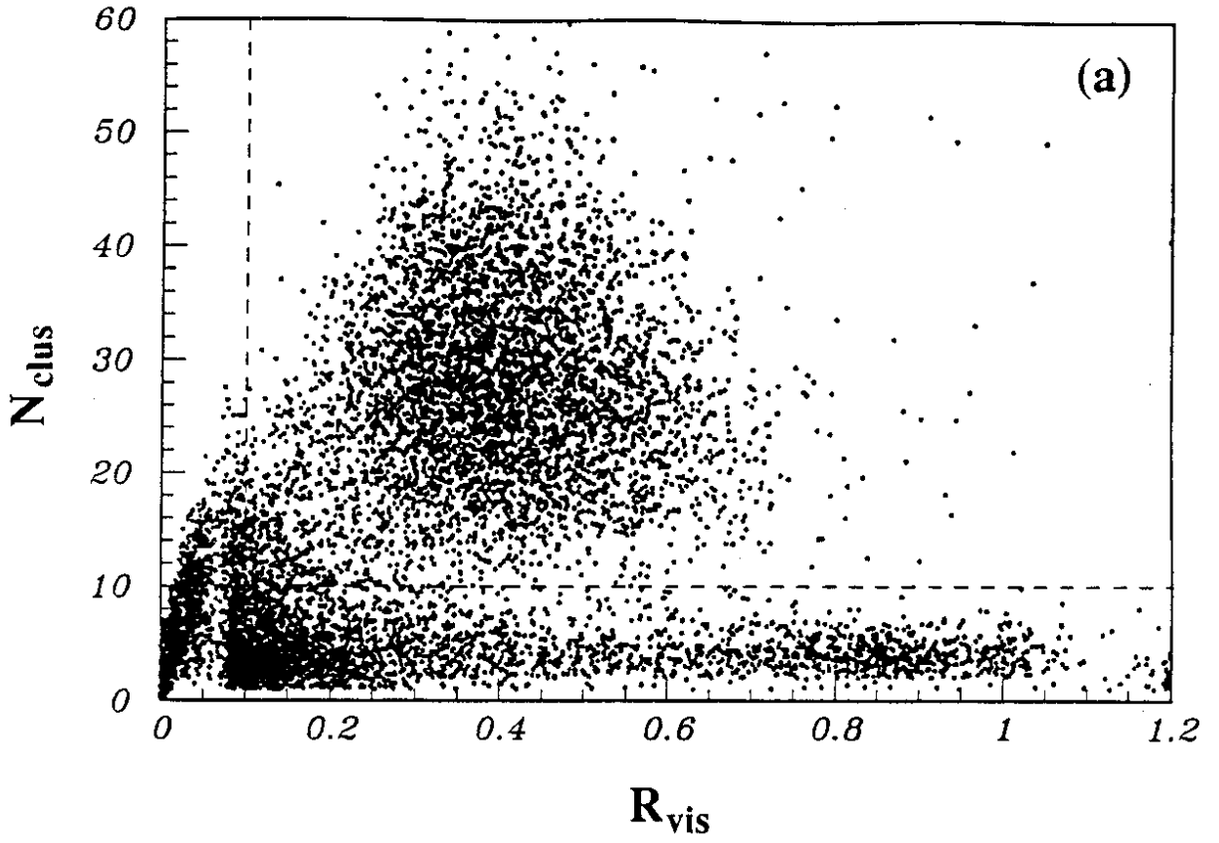
(a)
60
50
40
30
20
10
0
N_{clus}
0
0.2
0.4
0.6
0.8
1
1.2
R_{vis}

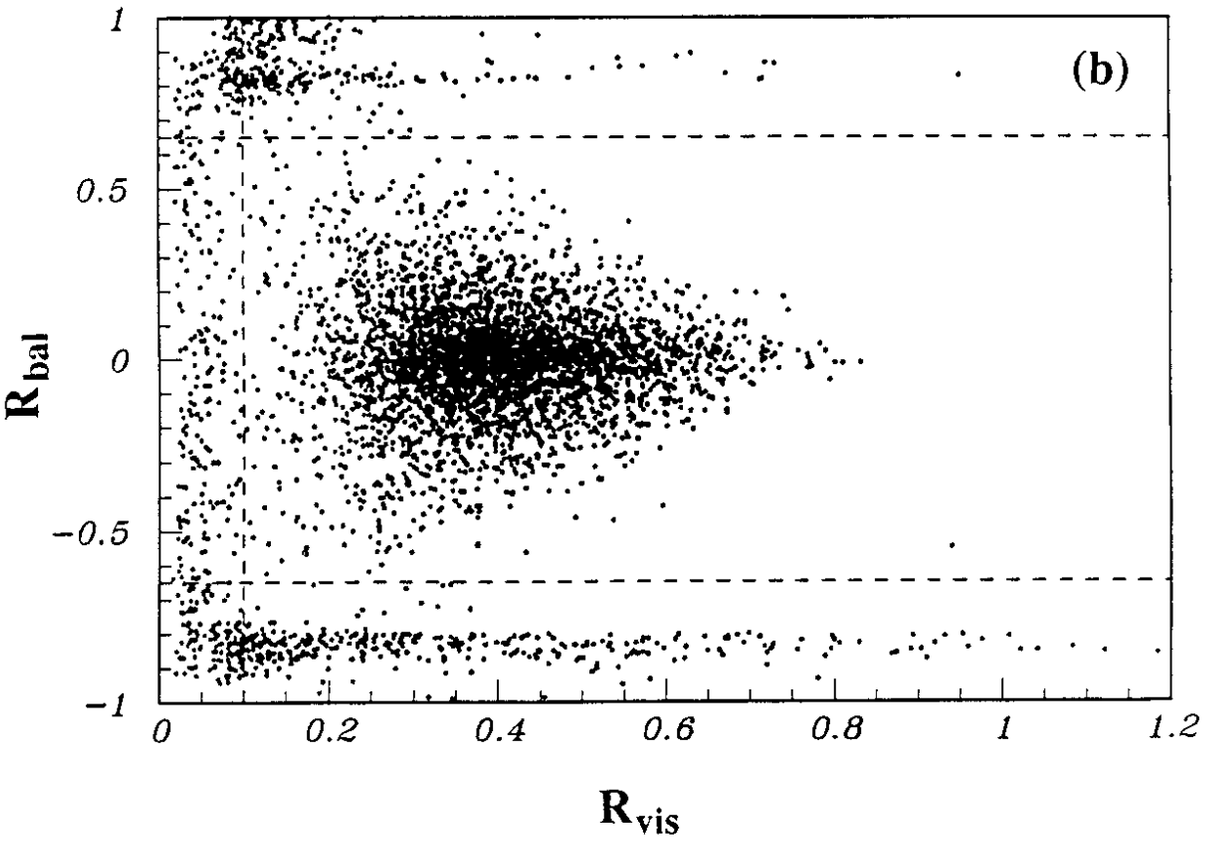
(b)
1
0.5
0
−0.5
−1
R_{bal}
0
0.2
0.4
0.6
0.8
1
1.2
R_{vis}

Fig. 1

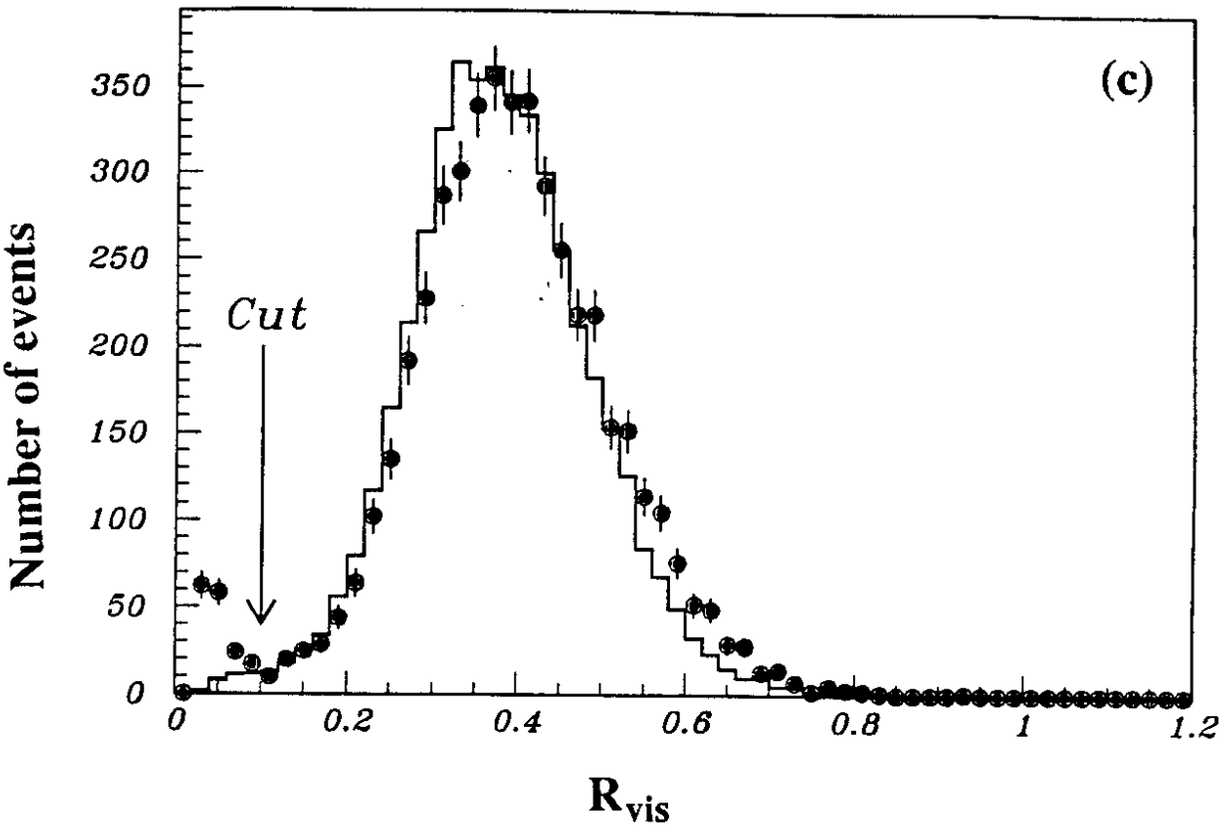
(c)
Number of events
350
300
250
200
150
100
50
0
Cut
0
0.2
0.4
0.6
0.8
1
1.2
R_{vis}

Fig. 1

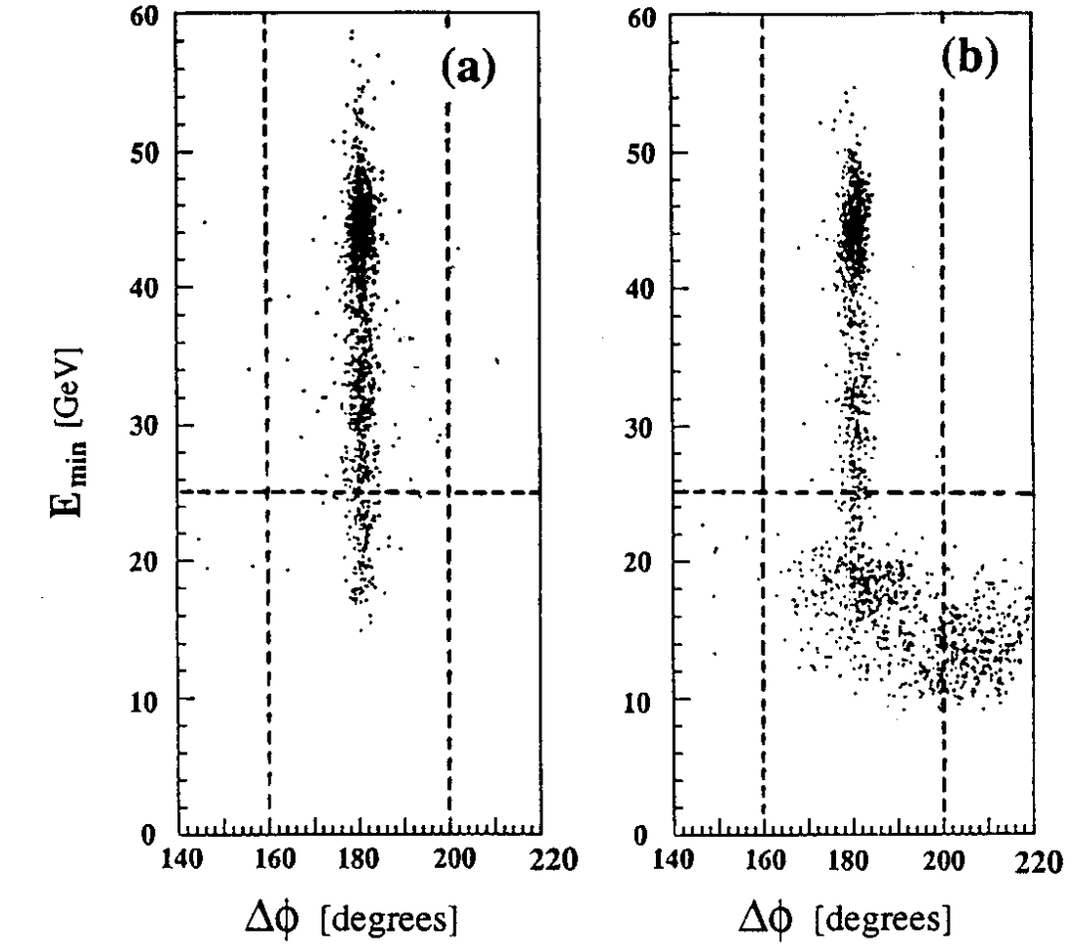
(a)
(b)
E_{min} [GeV]
$\Delta\phi$ [degrees]
$\Delta\phi$ [degrees]
0
10
20
30
40
50
60
140
160
180
200
220

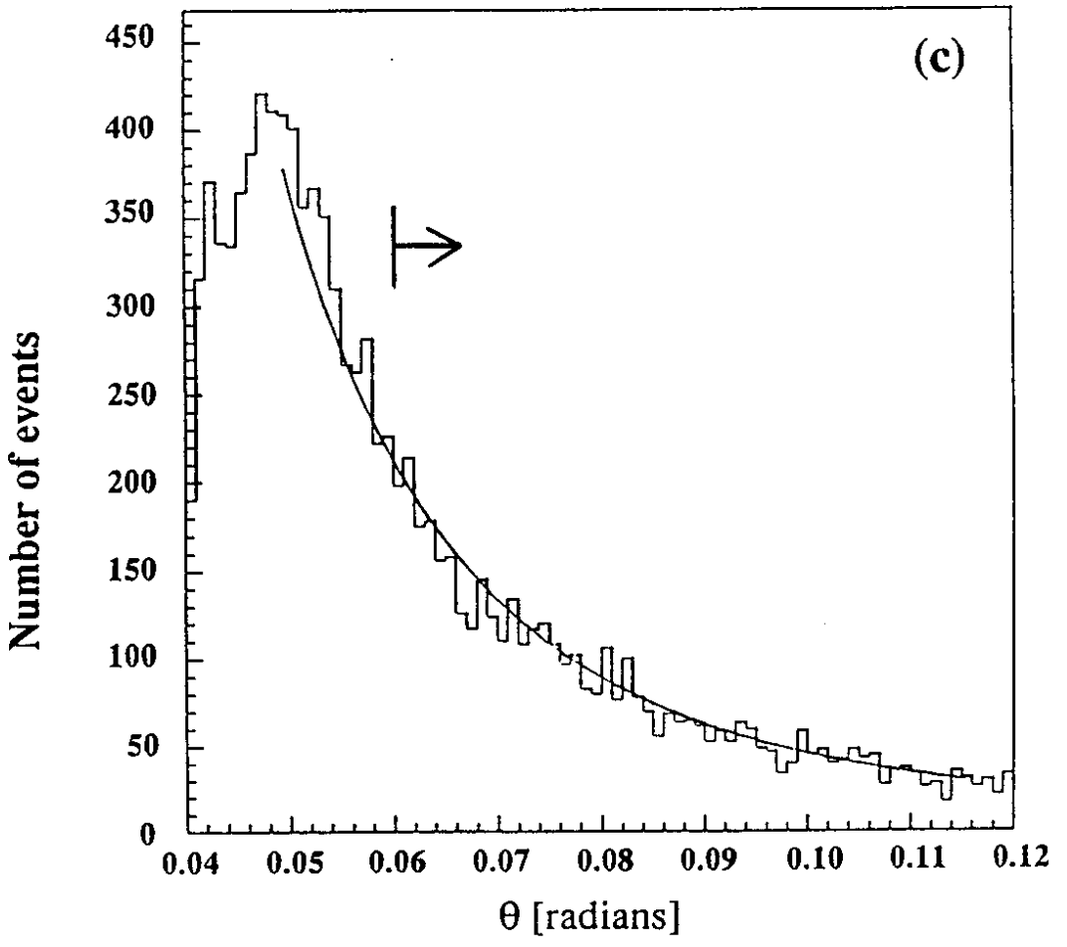
(c)
Number of events
θ [radians]
0
50
100
150
200
250
300
350
400
450
0.04
0.05
0.06
0.07
0.08
0.09
0.10
0.11
0.12

Fig. 2

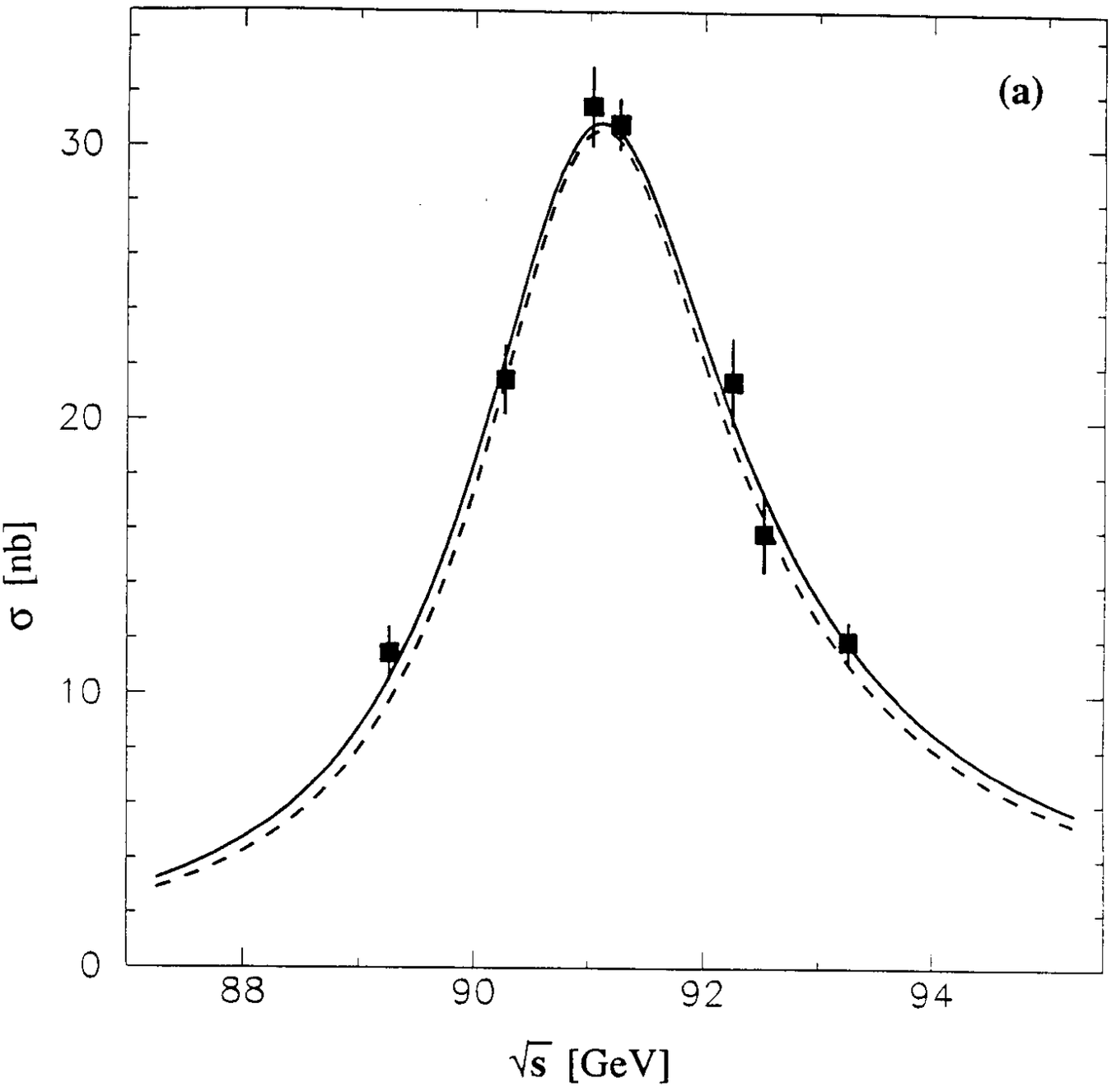

Fig. 3

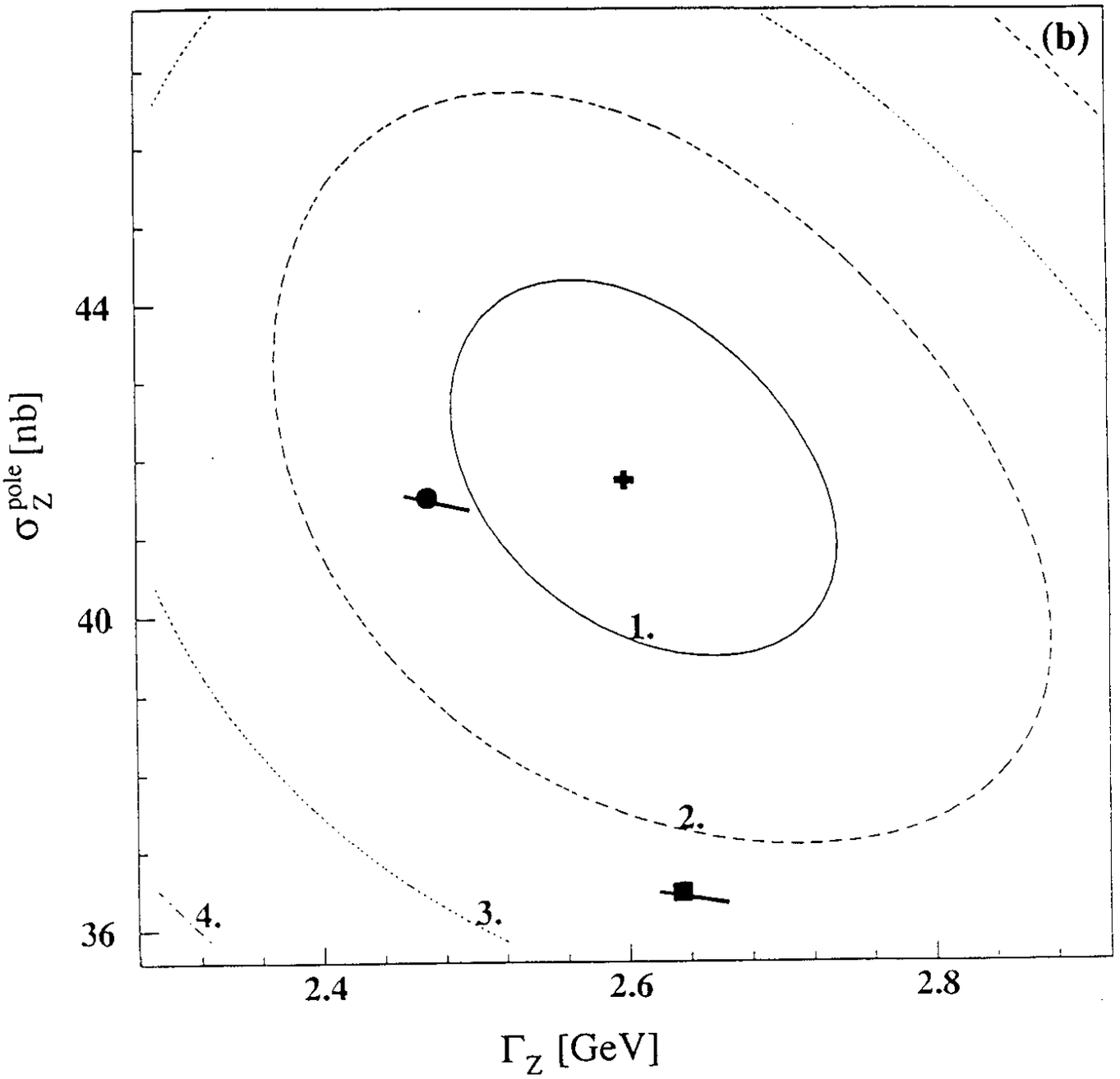

Fig. 3